

Experimental observation of slow light in photonic crystal coupled waveguides

Takashi Kawasaki, Daisuke Mori, and Toshihiko Baba*

*Yokohama National University, Department of Electrical and Computer Engineering,
79-5 Tokiwadai, Hodogayaku, Yokohama 240-8501, Japan*

*Corresponding author: baba@ynu.ac.jp

Abstract: We experimentally demonstrate wideband dispersion-free slow light in chirped photonic crystal coupled waveguides (PCCW). In unchirped PCCWs, the zero group velocity can occur at an inflection point of a photonic band of even symmetric mode. The even symmetric mode is selectively excited by connecting the device with input and output waveguides through optimized branch and confluence structures. In the device fabricated on SOI substrate, a large increase in group delay was observed with a maximum group index of 140 and the zero group velocity dispersion at the inflection point. Photonic bands estimated from the group delay characteristics corresponded to calculated ones. In the chirped PCCWs, the group velocity dispersion was internally compensated and the nearly constant group index of 50–60 was obtained in a wavelength bandwidth of 10 nm. The dispersion compensation was also confirmed through the transmission measurement of sub-ps optical pulses.

©2007 Optical Society of America

OCIS codes: (230.3990) Microstructure devices; (230.3120) Integrated optics device

References and links

1. T. Baba, N. Fukaya, and J. Yonekura, "Observation of light transmission in photonic crystal waveguides with bends," *Electron. Lett.* **35**, 654-655 (1999).
2. T. Baba, A. Motegi, T. Iwai, N. Fukaya, Y. Watanabe and A. Sakai, "Light propagation characteristics of straight single line defect optical waveguides in a photonic crystal slab fabricated into a silicon-on-insulator substrate," *Japan. Quantum. Electron.* **38**, 743-752 (2002).
3. S. J. McNab, N. Moll, and Y. Vlasov, "Ultra-low loss photonic integrated circuit with membrane-type photonic crystal waveguides," *Opt. Express* **11**, 2927-2939 (2003).
4. Y. Sugimoto, Y. Tanaka, N. Ikeda, Y. Nakamura, K. Asakawa, and K. Inoue, "Low propagation loss of 0.76 dB/mm in GaAs-based single-line-defect two-dimensional photonic crystal slab waveguides up to 1 cm in length," *Opt. Express* **12**, 1090-1096 (2004).
5. E. Kuramochi, M. Notomi, S. Hughes, A. Shinya, T. Watanabe, and L. Ramunno, "Disorder-induced scattering loss of line-defect waveguides in photonic crystal slabs" *Phys. Rev. B* **72**, 161318 (2005).
6. M. Notomi, K. Yamada, A. Shinya, J. Takahashi, C. Takahashi, and I. Yokohama, "Extremely large group-velocity dispersion of line defect waveguides in photonic crystal slabs," *Phys. Rev. Lett.* **87**, 253902 (2001).
7. K. Inoue, N. Kawai, Y. Sugimoto, N. Carlsson, N. Ikeda, and K. Asakawa, "Observation of small group velocity in two-dimensional AlGaAs-based photonic crystal slabs" *Phys. Rev. B* **65**, 121308 (2002).
8. T. Asano, K. Kiyota, D. Kumamoto, B-S. Song, and S. Noda, "Time-domain measurement of picosecond light-pulse propagation in a two-dimensional photonic crystal-slab waveguide," *Appl. Phys. Lett.* **84**, 4690-4692 (2004).
9. Yu. A. Vlasov, M. O'Boyle, H. F. Hamann and S. J. McNab, "Active control of slow light on a chip with photonic crystal waveguides," *Nature* **438**, 65-69, (2005).
10. H. Gersen, T. J. Karle, R. J. P. Engelen, W. Bogaerts, J. P. Korterik, N. F. van Hulst, T. F. Krauss, and L. Kuipers, "Real-space observation of ultraslow light in photonic crystal waveguides," *Phys. Rev. Lett.* **94**, 073903 (2005).
11. K. Kiyota, T. Kise, N. Yokouchi, T. Ide, and T. Baba, "Various low group velocity effects in photonic crystal line defect waveguides and their demonstration by laser oscillation," *Appl. Phys. Lett.* **88**, 201904 (2006).
12. D. Mori and T. Baba, "Dispersion-controlled optical group delay device by chirped photonic crystal waveguides," *Appl. Phys. Lett.* **85**, 1101-1103 (2004).
13. T. Baba and D. Mori, "Slowlight engineering in photonic crystals," *J. Phys. D: Appl. Phys.* **40**, 2659-2665 (2007).

14. A. Sakai, I. Kato, D. Mori and T. Baba, "Anomalous low group velocity and low dispersion in simple photonic crystal line defect waveguides," IEEE/LEOS Annual Meet., ThQ5 (2004).
15. A. Y. Petrov and M. Eich, "Zero dispersion at small group velocities in photonic crystal waveguides," Appl.Phys. Lett. **85**, 4866-4868 (2004).
16. M. L. Povinelli, S. G. Johnson, and J. D. Joannopoulos, "Slow-light, band-edge waveguides for tunable time delays," Opt. Express **13**, 7145-7159 (2005).
17. D. Mori, and T. Baba, "Wideband and low dispersion slow light by chirped photonic crystal coupled waveguide," Opt. Express **13**, 9398-9408 (2005).
18. R. J. P. Engelen, Y. Sugimoto, Y. Watanabe, J. P. Korterik, N. Ikeda, N. F. van Hulst, K. Asakawa, and L. Kuipers, "The effect of higher-order dispersion on slow light propagation in photonic crystal waveguides," Opt. Express **14**, 1658-1672 (2006).
19. C. E. Finlayson, F. Cattaneo, N. M. B. Perney, J. J. Baumberg, M. C. Netti, M. E. Zoorob, M. D. B. Charlton, and G. J. Parker, "Slow light and chromatic temporal dispersion in photonic crystal waveguides using femtosecond time of light," Phys. Rev. **E73**, 016619 (2006).
20. L. H. Frandsen, A. V. Lavrinenko, J. Fage-Pedersen, and P. I. Borel, "Photonic crystal waveguides with semi-slow light and tailored dispersion properties," Opt. Express **14**, 9444-9450 (2006).
21. M. D. Settle, R. J. P. Engelen, M. Salib, A. Michaeli, L. Kuipers, and T. F. Krauss, "Flatband slow light in photonic crystals featuring spatial pulse compression and terahertz bandwidth," Opt. Express **15**, 219-226 (2007).
22. S. C. Huang, M. Kato, E. Kuramochi, C. P. Lee and M. Notomi, "Time-domain and spectral-domain investigation of inflection-point slow-light modes in photonic crystal coupled waveguides," Opt. Express **15**, 3543-3549 (2007).
23. D. Mori, S. Kubo, H. Sasaki, and T. Baba, "Experimental demonstration of wideband dispersion-compensated slow light by a chirped photonic crystal directional coupler," Opt. Express **15**, 5264-5270 (2007).
24. S. Kubo, D. Mori and T. Baba, "Demonstration of low-group-velocity and Low-dispersion photonic crystal waveguide," IEEE/LEOS Int. Conf. Group IV Photon., WP35 (2007).
25. Y. Watanabe, Y. Sugimoto, N. Ikeda, N. Ozaki, A. Mizutani, Y. Takata, Y. Kitagawa and K. Asakawa, "Broadband waveguide intersection with low-crosstalk in two-dimensional photonic crystal circuits by sing topology optimization," Opt. Express **14**, 9502-9507 (2006).

1. Introduction

Optical buffers will be a key component for photonic routers in future transparent optical networks. For this reason, compact optical delay lines based on slow light having an ultra low group velocity v_g have been extensively studied. Photonic crystal slab line defect waveguides (PCWs) [1-5] generate slow light, utilizing large structural dispersion at the photonic band edge [6-11]. Compared with those generated by using large material dispersion in atomic systems, the slow light in the PCWs has the advantage that it is generated in a solid-state device at room temperature. However, due to its narrow operating bandwidth and large group velocity dispersion (GVD), the slow light at the band edge cannot be straightforwardly used for optical buffering. Because of this reason, we have theoretically discussed the generation of useful slow light whose bandwidth is appropriately expanded and GVD is suppressed [12,13], and some groups have investigated various device structures and photonic bands in these years [14-24].

A solution we have proposed to overcome the above-mentioned problems is a directional coupler consisting of two PCWs of the same type [17], which has a symmetric even mode that exhibits the zero v_g condition at an inflection point other than the band edge. This mode is selectively excited by connecting the directional coupler and the input and output (I/O) PCWs through a branch and confluence. We named this device photonic crystal coupled waveguides (PCCWs). By ensuring that higher and lower frequency bands are symmetric with respect to the inflection point, opposite GVD characteristics are realized, and zero v_g and the zero GVD condition is satisfied at the inflection point. By employing a chirped structure having gradually varying parameters, the inflection point is shifted over a bandwidth determined by the range of the chirping. Consequently, the slow light is obtained in the bandwidth and the GVD in the bandwidth is compensated in the device. Compared with other structures proposed and studied for useful slow light, design flexibility of the group velocity and the bandwidth is an important advantage of this device. We theoretically demonstrated stopping

of an optical pulse in such chirped PCCWs. Recently, a preliminary experiment was reported, demonstrating the fabrication of unchirped PCCWs on a silicon-on-insulator (SOI) substrate and the observation of a low v_g of $0.017c$ [22]. In that study, a Si-wire branch and confluence were used to excite the even mode. However, electromagnetic fields of the even mode in the PCCW are not necessarily localized inside the two waveguides, but rather a large intensity occurs at the inter-waveguide spacing particularly on the low frequency side. Thus the branch and confluence did not provide a high excitation efficiency of the even mode and a low insertion loss. For this reason, the frequency band of the group delay measurement was limited and the inflection point was not clearly determined. Besides, the wideband GVD-compensated slow light in the chirped PCCWs has not been demonstrated yet.

In the present study, we fabricated PCCWs having a PCW-based optimized branch and confluence and evaluated its detailed transmission spectrum, group delay, and GVD characteristics. For the unchirped device, we observed a higher group index $n_g \equiv c/v_g$ and the zero GVD condition at the inflection point, and obtained a reasonable correspondence between the experimentally measured and theoretically calculated photonic bands. Moreover, we successfully observed the wideband GVD-compensated slow light in a chirped device through the group delay measurement and the transmission of ultrashort optical pulses.

2. Design and Fabrication

We first fabricated air-bridge unchirped PCCWs on a SOI substrate having a $0.213\text{-}\mu\text{m}$ -thick top Si layer using e -beam lithography, SF_6 inductively coupled plasma etching, and HF wet etching. A scanning electron microscope image of the device is shown in Fig. 1. I/O PCWs were connected to the PCCWs, and a rectangular groove was placed at the end of the output waveguide to pick up the transmitted light. The target operation wavelength was set around $1.55\text{ }\mu\text{m}$, and the lattice constant a was fixed at $0.46\text{ }\mu\text{m}$. Also, the hole diameter $2r_1$ was $0.24\text{ }\mu\text{m}$ and one row of holes outside of each waveguide was shifted by $0.01\text{ }\mu\text{m}$. The hole diameter of the middle row of holes in the PCCW, $2r_2$, was varied between samples from 0.34 to $0.38\text{ }\mu\text{m}$. Figure 2(a) shows the photonic band diagram calculated for such a three-dimensional (3D) device model. When $2r_2 = 0.36\text{ }\mu\text{m}$, the zero v_g and zero GVD condition appears for the even mode band of the transverse-electric-like (TE-like) polarization. The I/O PCWs are required to have a transmission spectrum that overlaps with that of the even mode of the PCCWs. The band calculation indicated that this condition is satisfied when $2r_1$ of the I/O PCWs is $0.24\text{ }\mu\text{m}$ and their channel width is $0.08\text{ }\mu\text{m}$ narrower than the standard width of the single line defect PCW. In the experiment, we tested various different channel widths and observed the lowest insertion loss in the I/O PCW whose channel width was $0.07\text{-}\mu\text{m}$ narrower than the standard width. So, we employed this width in subsequent experiments. The lengths of the PCCWs, L_c , and that of output PCW, L_o , were $300\text{ }\mu\text{m}$ and $25\text{ }\mu\text{m}$, respectively.

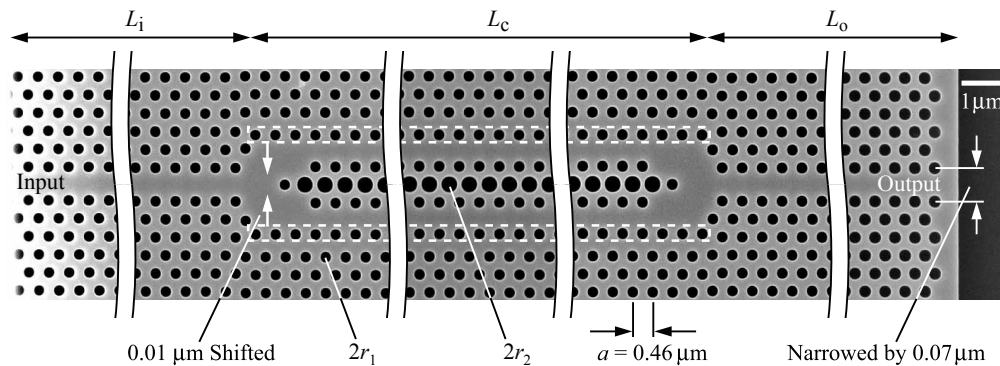


Fig. 1. Scanning electron microscope image of fabricated device.

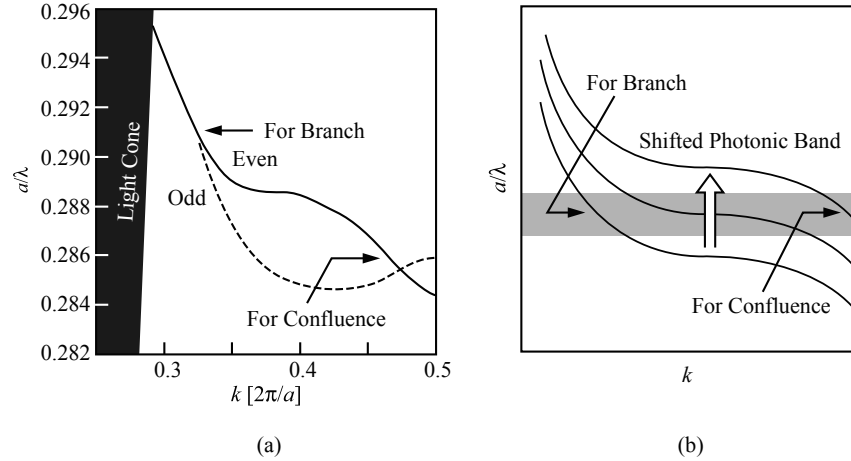


Fig. 2. Photonic band of a PCCW for the TE-like polarization. (a) Calculated band for $2r_2 = 0.36 \mu\text{m}$. Arrows indicate normalized frequencies used for optimizing the branch and confluence. (b) A schematic showing the band shift in a chirped structure.

The length of the input PCW, L_i , was determined by the cleavage of the sample, and typically $50 \mu\text{m}$.

Optimization of the branch and confluence connecting the PCCW with I/O PCWs is important for achieving low reflection loss and high transmission efficiency. In particular, the suppression of the reflection is important for reducing unwanted internal resonance. We have already reported some example structures designed using the 2D finite-difference time-domain (FDTD) method [17]. In a preliminary experiment, however, we noticed that these structures were not optimum for achieving low out-of-plane radiation loss in the actual 3D device. In this study, we performed a 3D FDTD calculation to further optimize parameters. The goal of this study is to generate GVD-compensated slow light in a chirped device, as described in Section 4. Figure 2(b) schematically shows the shift in the even mode band induced by using a chirped structure. Let us consider the situation in which input optical signals have a frequency bandwidth indicated by the gray band in this figure and the photonic band is shifted according to bandwidth. The I/O PCWs are then connected to the PCCW by the branch and confluence in the positive and negative GVD regions, respectively. We investigated optimum structures for achieving a low reflectance R and a high transmittance T at the normalized frequency $a/\lambda = 0.291$ and 0.286 of Fig. 2(a), which correspond to the positive and negative GVD regions, respectively. The branch and confluence were designed to be symmetric with respect to each other. If the simulation model were identical to the actual device in size, huge computational facilities would be required. We shortened the length of the PCCW, L_c , to be $49a$ and those of I/O PCWs, L_i and L_o , to be $19a$ in the mode. Figure 3 shows R and T calculated for three different types of branches and confluences; they are very sensitive to the arrangement of holes. All the structures give a low R and relatively high T at $a/\lambda = 0.291$. The reason that $T+R < 100\%$ should be the out-of-plane scattering loss. Structure III simultaneously give a low R and high T at $a/\lambda = 0.286$. It may be possible to further improve the transmission characteristics using topology optimization of the structure [25], which is a future issue of this device. Intensity distributions of guided light at these a/λ (the square of the component of the magnetic field perpendicular to the surface, H_z^2) were calculated using the FDTD method, as shown in Fig. 4. Light is smoothly splitted, transmitted and confluenced in this device.

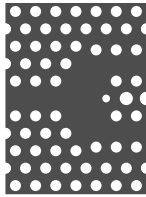
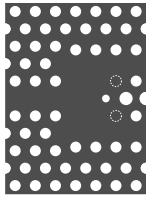
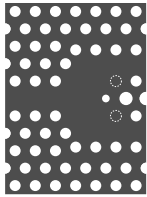
		I	II	III
a/λ				
0.291	R	0.5 %	2.8 %	0.5 %
	T	78 %	65 %	78 %
0.286	R	24 %	30 %	4.7 %
	T	60 %	61 %	88 %

Fig. 3. Calculation results for the reflectance R and transmittance T for three types of branches and confluences.

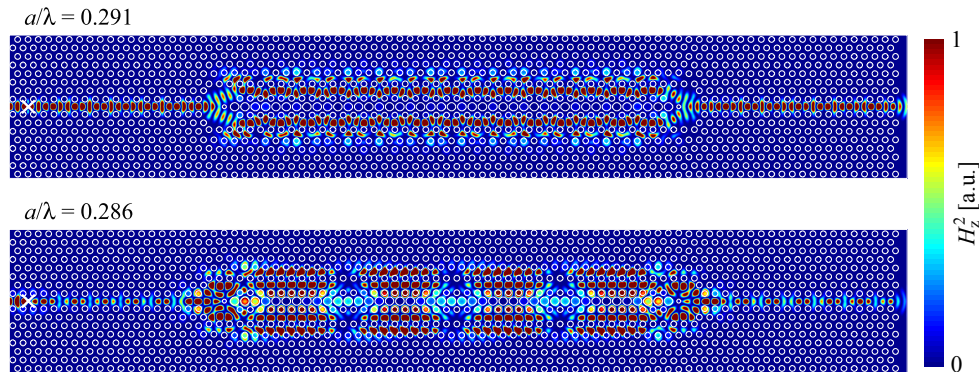


Fig. 4. Light propagation (H_z^2 distribution) simulated for structure III in Fig. 3 by 3D FDTD method. White cross on the left side represents the excitation point.

3. Measurement

We used an optical network analyzer (Advantest Q7750) to measure the transmission and group delay spectra. The group delay Δt was obtained by the modulation phase shift method; the phase shift $\Delta\phi$ of tunable laser light was sinusoidally modulated at $f = 3$ GHz and was detected between the I/O ends of the device, and Δt was obtained from the relation $2\pi f\Delta t = \Delta\phi$. The group index n_g of the PCCWs was evaluated as $[c\Delta t - (L_r + L_o)n_g^{(PCW)}]/L_c$, where the group index of I/O PCWs, $n_g^{(PCW)}$, was assumed to be 10. The measurement was carried out at wavelength intervals of 0.05 nm. However, data points at some wavelengths were not obtained since their transmission intensities were not sufficiently high to allow the phase shift to be measured. The results are shown in Fig. 5. It also shows experimentally obtained red data points for the photonic band which were obtained from the relation $n_g = c\Delta k/\Delta\omega$, and compared with the black data points that were obtained theoretically (solid line: even mode, dashed line: odd mode). Here, each theoretical line is shifted slightly so that it matches the transmission spectrum. The results are clearly sensitive to the value of $2r_2$. When $2r_2 \geq 0.38$ μm , the transmission band on the long wavelength side disappeared. This can be explained from the even mode band shifting to the short wavelength side. This means that the odd mode band, which extends over the whole wavelength range, was not excited, and only the even

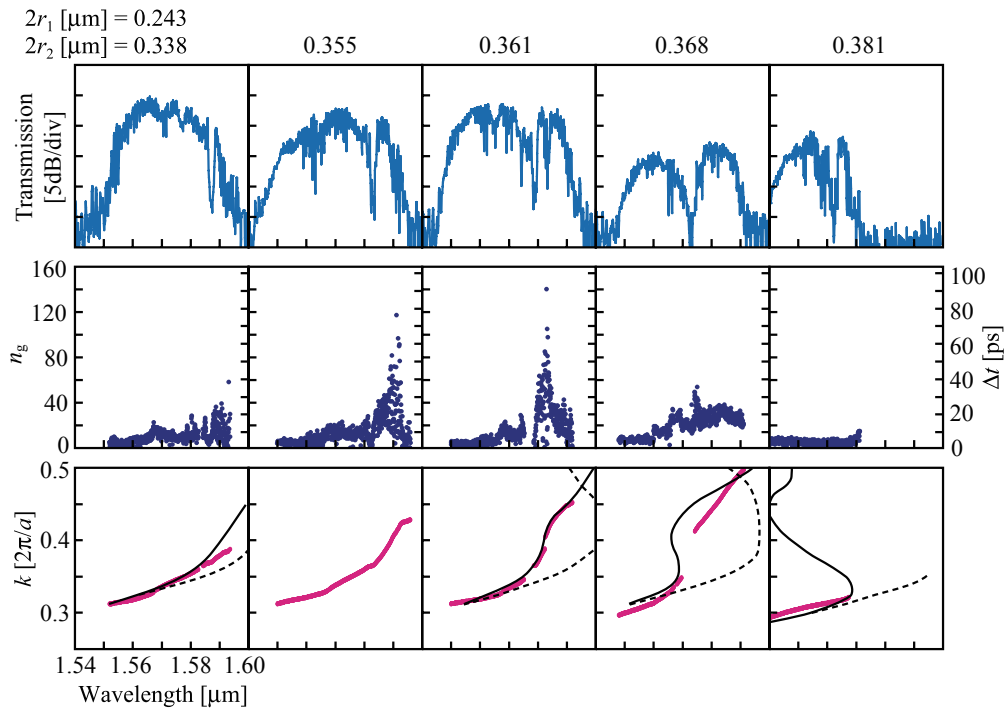


Fig. 5. Transmission spectrum, group index and group delay, and photonic band of unchirped PCCWs. Red and black data points of the photonic band denote experimentally and theoretically determined values, respectively. The solid line and dashed line indicate the even mode and the odd mode, respectively.

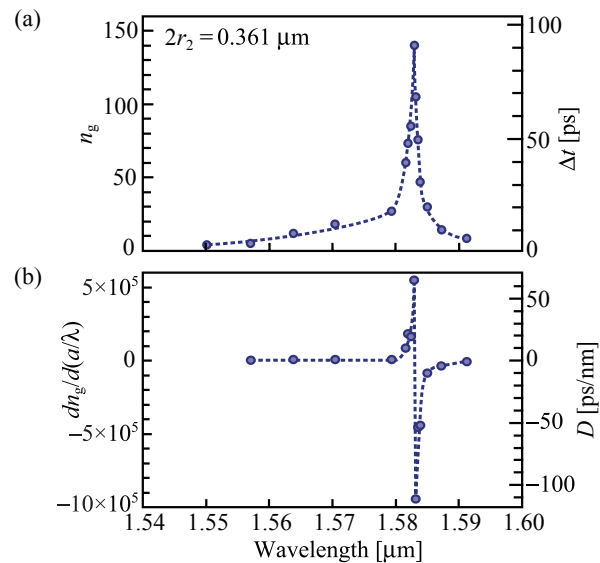


Fig. 6. GVD characteristics. (a) Sampled plots enveloping the group index and delay time characteristics for $2r_2=0.361 \mu\text{m}$ in Fig. 5. (b) GVD evaluated from (a).

mode propagated in the fabricated PCCW. When $2r_2 \leq 0.34 \mu\text{m}$, n_g ranged from 5 – 20. But when $2r_2 = 0.35 - 0.37 \mu\text{m}$, a large peak appeared that had a maximum of $n_g = 140$ at $2r_2 = 0.36 \mu\text{m}$. This peak is thought to correspond to the zero v_g condition of the flat band. At this peak wavelength, a small dip caused by the large n_g was observed in the transmission spectrum. Another large dip was also observed, although no marked changes appeared in the group delay and group index. A possible explanation for this large dip is a particularly severe mode mismatch between the PCCWs and I/O PCWs at the branch and confluence.

The theoretical and experimental bands approximately correspond with each other. At $2r_2 = 0.368 \mu\text{m}$, n_g exhibits two peaks, indicating that the band is winding like the calculated one. Under this condition, light is supposed to propagate by multiple modes. Therefore, the wavenumber k is not uniquely determined, and so the band curve between two peaks cannot be obtained. Figure 6(a) shows some selected plots enveloping the group delay characteristics at $2r_2 = 0.361 \mu\text{m}$, and Fig. 6(b) shows the corresponding GVD characteristics. Here, the normalized GVD coefficient $dn_g/d(a/\lambda)$ and absolute value of GVD coefficient D are plotted along the ordinate. A low dispersion was found for wavelengths far from the peak. Near the peak indicating the inflection point, the dispersion rapidly changes from a positive to a negative value, and just at the peak wavelength, the low v_g and the zero GVD condition were obtained simultaneously.

4. Chirped structure

For the demonstration of wideband GVD-compensated slow light, the same design as in Fig. 1 was employed except for $2r_1$. We linearly changed $2r_1$ along the PCCWs of $L_c = 250 \mu\text{m}$ from $0.25-0.27 \mu\text{m}$ by controlling the exposure time of the e -beam lithography. The center hole diameter $2r_2$ was fixed so that the shape of the even mode band did not change along the waveguide.

Transmission intensity, group index, and group delay spectra of the fabricated device are shown in Fig. 7(a) and (b). Since the internal resonance was enhanced by a fluctuation in $2r_1$

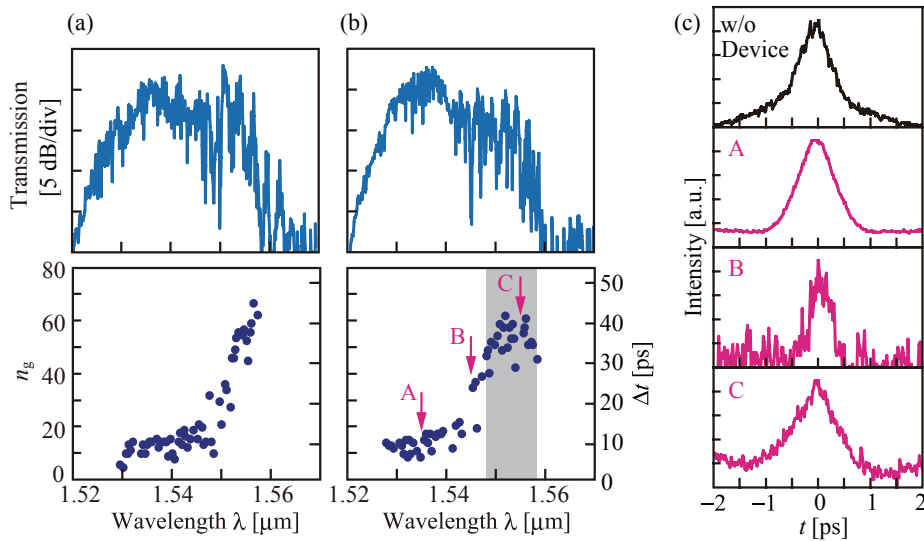


Fig. 7. Measured transmission characteristics in chirped PCCWs. Transmission spectra, group index and group delay for (a) $2r_2 = 0.345 \mu\text{m}$ and (b) $2r_2 = 0.367 \mu\text{m}$. (c) Autocorrelation traces of transmitted optical pulse. A, B and C correspond to wavelengths in (b).

of several nanometers, the phase analysis as described in [23] was applied to evaluate n_g of the PCCWs, neglecting the resonant effect. When $2r_2 = 0.345 \mu\text{m}$, the even mode band of the PCCW is like a band edge of the PCW, as expected from the results in Fig. 5. Therefore, n_g increased monotonically near the band edge even with the chirped structure. On the other hand, when $2r_2 = 0.367 \mu\text{m}$, the bandwidth of the slow light was expanded, because the symmetric peak of n_g in the unchirped device was evened out by the band shift in the chirped structure. The average n_g of the slow light was 50–60 in a wavelength bandwidth of 10 nm.

To further confirm the GVD compensation in the device, 0.8-ps-wide optical pulses from mode-locked tunable fiber laser was incident to the device. Auto-correlated waveforms of output pulses at different center wavelengths are shown in Fig. 7(c). Symbols A, B, and C denote different center wavelengths of the pulses and correspond to those in Fig. 7(b). At wavelength A, almost the same pulse width as the case without device was observed because of the low GVD. At wavelength B, the GVD was not compensated, so the pulse was disrupted and weakened. At wavelength C, the pulse shape was recovered because of the GVD compensation.

5. Summary

We fabricated PCCWs on a SOI substrate, which were connected to input and output waveguides by an optimized branch and confluence, respectively. Unique transmission and group delay characteristics indicating even mode propagation were clearly observed. By optimizing the hole diameters of the middle row of the coupled waveguides, the group delay exhibited a large peak with a maximum group index of 140. From the symmetric spectral shape of the peak, a low group velocity and the zero GVD condition at the inflection point were confirmed. The photonic band evaluated from the measured dispersion characteristics approximately corresponded to the calculated one. We also fabricated PCCWs with a hole diameter chirping and successfully observed the group index of 50–60 in a wavelength bandwidth of 10 nm. The GVD compensation in the device was also confirmed from the sub-ps optical pulse transmission; the pulse shape was well maintained even on the slow light condition. Thus, the wideband dispersion-free slow light was clearly demonstrated in this study.

Acknowledgment

This work was supported by The Core Research for Evolutional Science and Technology (CREST) Project of Japan Science and Technology (JST), a Grant-In-Aid for “Priority Research” from the Ministry of Education, Culture, Sports, Science and Technology (MEXT), The Kurata Memorial Hitachi Science and Technology Foundation, The Telecommunications Advancement Foundation, and SCAT Technology Research Foundation.